Available online at www.sciencedirect.com
ScienceDirect
Sensors and Actuators A 133 (2007) 272–277
SENSORS AND ACTUATORS A PHYSICAL
www.elsevier.com/locate/sna

A high-performance MEMS capacitive strain sensing system

Wen H. Ko *, Darrin J. Young, Jun Guo, Michael Suster, Hung-I Kuo, N. Chaimanonart

Electrical Engineering and Computer Science Department, Case Western Reserve University, 10900 Euclid Ave, Cleveland, OH 44106, USA

Received 8 July 2005; received in revised form 10 January 2006; accepted 7 March 2006
Available online 25 July 2006

Abstract

This paper describes the design of a functional strain sensing module with large dynamic range (80 dB), DC to 10 kHz response, high resolution, and mini size for industrial applications, such as the rolling-element bearings research. The design of the MEMS capacitive strain sensor employs mechanical amplifications of package design and buckle beams as well as the linear differential comb capacitor. The sensor is interfaced with a low noise charge amplifier, mixer, and filter circuits to provide an analog output that demonstrated a resolution of 0.09 microstrains with a maximum range of ±1000 microstrains. The sensor and the electronic circuits, including a temperature sensor, can be integrated on a chip, and packaged as a small functional unit. Additional electronics were integrated with the interface circuit on the chip that provide A/D conversion, radio frequency power supply, and digital signal telemetry to a near-by control unit. Preliminary test results are compared with the design simulation.

Keywords: Strain sensors; Capacitive sensor; Mechanical gain in strain sensors; Functional strain sensing module; RF powered passive sensor module; Sensor telemetry system

1. Introduction

High-performance strain sensing functional modules consisting of sensors and interface electronics are highly desirable for advanced industrial applications, such as point-stress and torque sensing for ball-bearings, rotating shafts and blades, etc. Performance requirements with a resolution of 0.1 microstrains over a wide bandwidth and a dynamic range of 80 dB are demanded for these applications. Commercial metal foils and piezoresistive element strain sensors are inadequate for the high-performance applications [1,2]. Capacitive strain sensors have many advantages such as high sensitivity, low temperature dependence, low noise, large dynamic range, and potential monolithic integration with CMOS circuits [3].

In this paper, a novel capacitive MEMS strain sensor is matched to a low noise CMOS integrated interface sensing electronics to achieve the performance of resolution, dynamic range, and signal bandwidth desired, as a module with analog or digital outputs. Additional electronics were designed and integrated with the sensing electronic to power the strain sensing module and to provide a digital data telemetry link to the external RF powering and control unit. This second module can then be used as a passive sensor module for strain measurement on rotating shaft or other fast moving elements. The major design consideration of the sensor and the measured module performance are presented and agree closely with the design and simulated goals.

2. Sensor design

Strain sensors are widely used. Capacitive strain sensors have advantages in temperature drift, sensitivity, noise, and dynamic range, as compared to metal foil and piezoresistive sensors. Researches were reported to measure residual stresses utilizing mechanical amplification scheme [4] with a strain resolution of 10 microstrains. A novel high-performance capacitive strain sensor employing mechanical amplifications of packaging design and buckle beams suspension; and the comb structure for differential capacitive linear output is designed. These mechanical amplifications improve the sensor sensitivity and reduce sensitivity requirement and power dissipation on the interface circuits. Fig. 1 shows a simplified schematic of a capacitive MEMS strain sensor with buckle beams.

The device consists of three amplifying buckle beams, with comb fingers positioned at the structural center. The beams give mechanical amplification to the applied strain, and the sensor

* Corresponding author. Tel.: +1 216 368 4081; fax: +1 216 368 6039.
E-mail address: whk@cwru.edu (W.H. Ko).

0924-4247/$ – see front matter
doi:10.1016/j.sna.2006.06.015

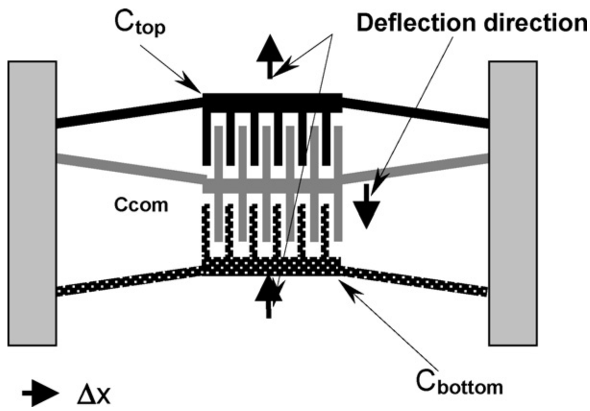

Fig. 1. Capacitive strain sensor.

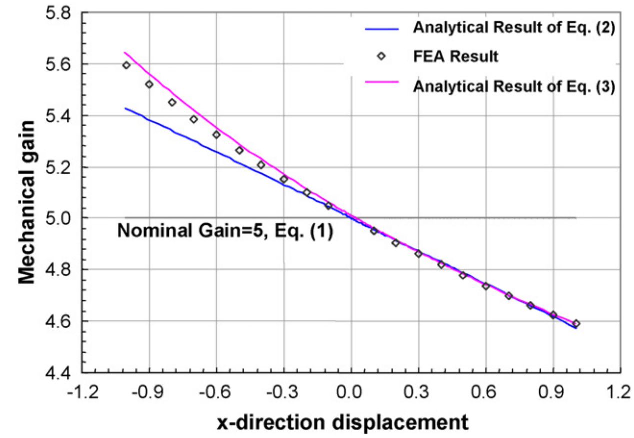

Fig. 3. A buckle beam strain sensor with differential output.

gives linear differential capacitive output as a measure of the applied strain, Δx.

A folded packaging frame structure also is used in the package of the capacitive sensor that provides a mechanical connection to the interface electronics. Furthermore, it gives an additional mechanical amplification, reduces the bonding attenuation, and achieves a high transverse strain rejection ratio as will be explained later.

Fig. 2 shows the principle of the buckle beam amplification architecture. An applied strain causes a small lateral displacement, Δx. With a small buckle angle, α, the center deflection of the beam, Δw, can be larger than Δx thus resulting in a mechanical gain.

For very small Δx, the angle, α, can be considered constant. The mechanical gain is constant. The sensor output is linear with strain input, as given in Eq. (1).

$$A_{\mathrm{mech}} = \frac{\Delta w}{\Delta x} \cong \frac{1}{2}\mathrm{ctg}\alpha \qquad (1)$$

However, as the Δx increases, the angle α change with the load can no more be omitted, which results in the non-linear property of the mechanical gain, as approximated,

$$A^{*}_{\mathrm{mech}} = \frac{1}{2\tan\alpha}\left[1 - \frac{1}{2\tan^2\alpha}\frac{\Delta x}{L}\right]. \qquad (2)$$

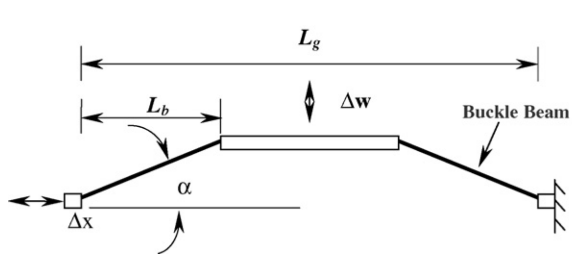

Fig. 2. Principle of a buckle beam amplification.

The complete analytical solution of the mechanical gain of the buckle beams is given by Eq. (3), one for tension and the other for compression.

$$A_{\mathrm{mech}} = \frac{\Delta w}{\Delta x} \cong \frac{2(\tan\alpha/k)\tan(kL/2) - h}{\tan^2\alpha[(\tan^2(kL/2)/4k)(-\sin(2kL) + 2kL) + (\sin(2kL) + 2kL/4k) - (\tan(kL/2)/2k)(\cos(2kL) - 1)]}$$
$$A_{\mathrm{mech}} = \frac{\Delta w}{\Delta x} \cong \frac{2(\tan\alpha/k)\tanh(kL/2) - h}{\tan^2\alpha[(\tanh^2(kL/2)/4k)(\sinh(2kL) - 2kL) + (\sinh(2kL) + 2kL/4k) - (\tanh(kL/2)/2k)(\cosh(2kL) - 1)]} \qquad (3)$$

A FEA simulation was also made. Fig. 3 shows the comparison of analytical and FEA stimulated results. FEA gives same result as Eq. (3), Eq. (2) gives an error about 2% at 1000 microstrain, tension. The parameters of the buckle beam used are: $L_g = 1000\ \mu\mathrm{m}$, $L_b = 300\ \mu\mathrm{m}$ and the buckle angle = 5.7°. The mechanical gain for a buckle beam is 5. For the sensor with two buckle beams as a set, the gain is 10. These results agree well with the experimental data observed on fabricated strain sensors.

The linear differential capacitive output can be obtained by employing sensing comb fingers as shown in Fig. 4. By designing comb drive fingers at the center beam as shown, for a compressive strain, the top, Cx^+, beam and bottom Cx^- beam will move up and the center beam will move down, resulting in a differential capacitance output signal with mechanical gain twice that of a single buckle beam set.

The device sensitivity and other performance were studied. They can be optimized by carefully selecting parameters such as

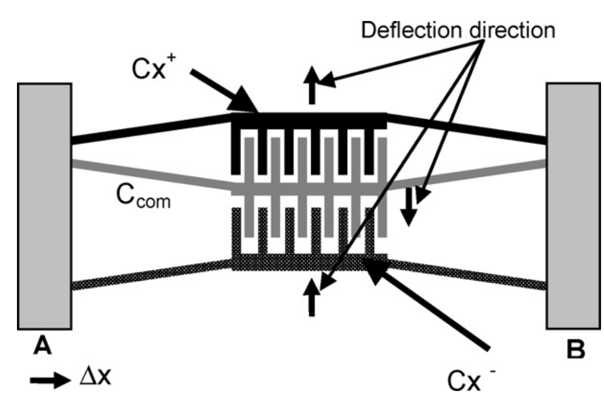

Fig. 4. A buckle beam strain sensor with differential output.

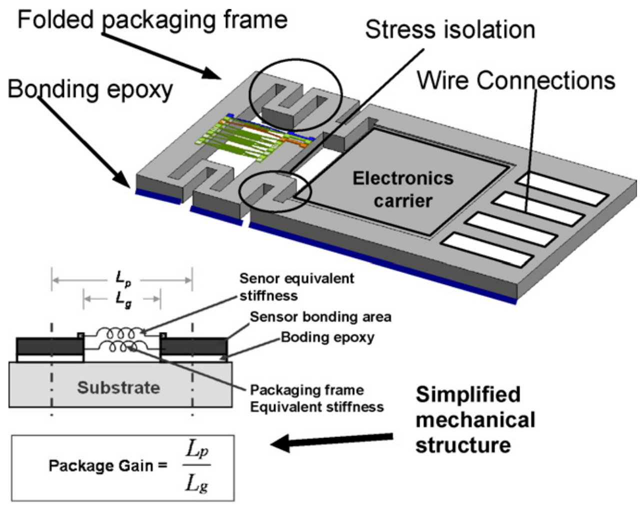

Fig. 5. Sensor on a packaged frame.

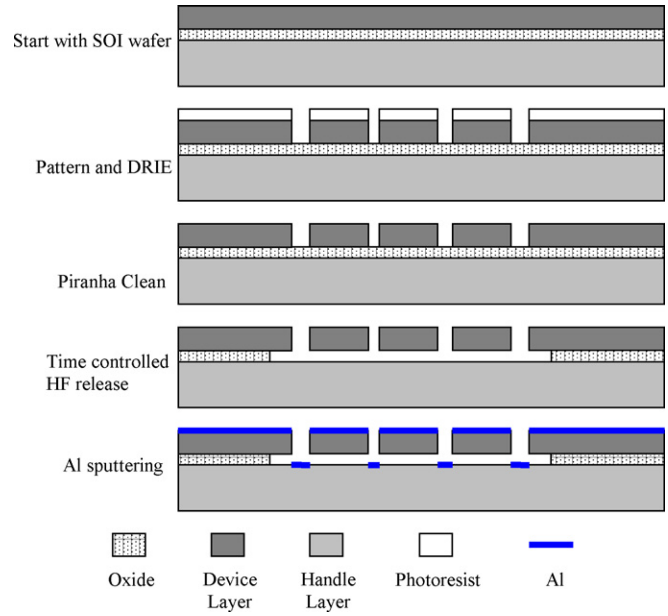

Fig. 6. Fabrication process flow chart.

buckling angle, fingers numbers, thickness and gap size, using the developed FEA simulation program. Optimized sensor has a buckle angle of 5.7°, a structural thickness of 20 μm, a minimum air gap size of 3.6 μm, and a lateral gauge length of 1 mm, a total number of 260 sensing fingers [5].

The sensor also employs novel packaging design with a folded frame as shown in Fig. 5. The sensor and the folded frame can be simplified as two springs. By carefully selecting the geometrical parameters, the stiffness of the two springs can be designed to be weak as compared to bonding area strength, thus achieving an additional mechanical gain, $A_p = L_p/L_g$, and minimizing the strain attenuation loss caused by the bonding adhesive interface [6].

A high transverse strain rejection ratio (the sensitivity ratio in *X* direction over that in *Y* direction) is also achieved due to the structural high transverse strength. The microstructure also employs a strain isolation scheme to minimize the interference strain introduced by the electronics carrier and wire connections.

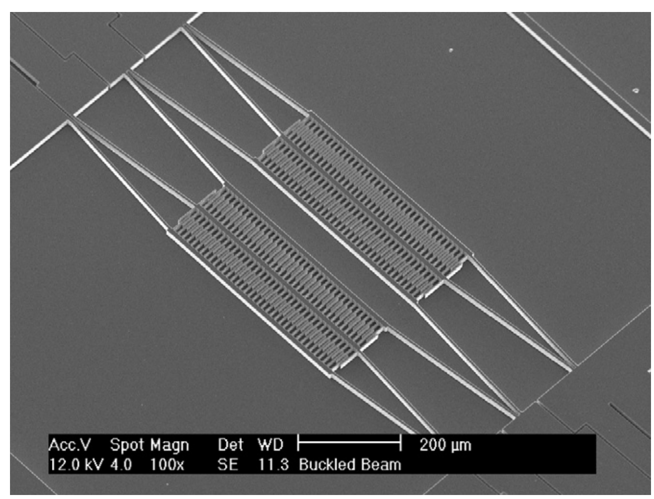

Fig. 7. SEM picture of a buckle beam strain sensor with two sets of buckled beams.

3. Fabrication and test result

A one-mask fabrication process, as shown in Fig. 6, was designed to verify the design and simulation results. The fabrication process started with a SOI wafer with device/oxide layer of 20/2 μm. The wafer was first patterned for a DRIE process, then diced, cleaned, and followed by a timed HF release process. A 200 Å Aluminum layer was then sputtered on the device to reduce the sensor series resistance and resistive thermal noise. The prototype fabrication achieved a yield close to 100% due to the simplicity of the design and fabrication process. An SEM picture of the sensor is shown in Fig. 7 with parameters given in Section 2.

The sensor was bonded on a stainless steel beam by epoxy, then measured using a three-point testing fixture developed for device testing [6]. The mechanical gain was determined by analyzing the captured optical images. Fig. 8 shows a typical characteristic curve of the sensor capacitance change versus the applied compressive strain. An overall differential mechanical

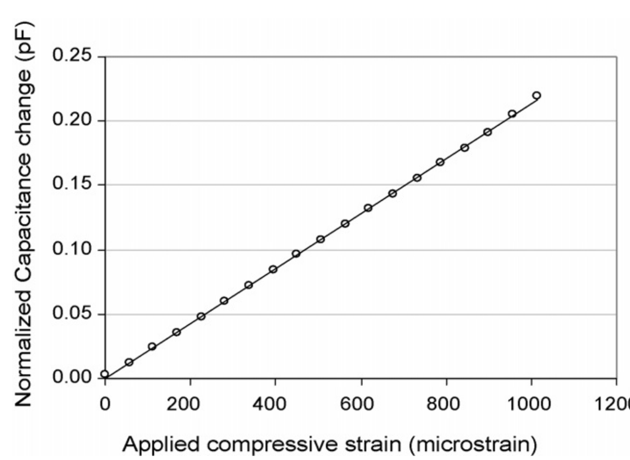

Fig. 8. Measured capacitance change as a function of the applied strain.

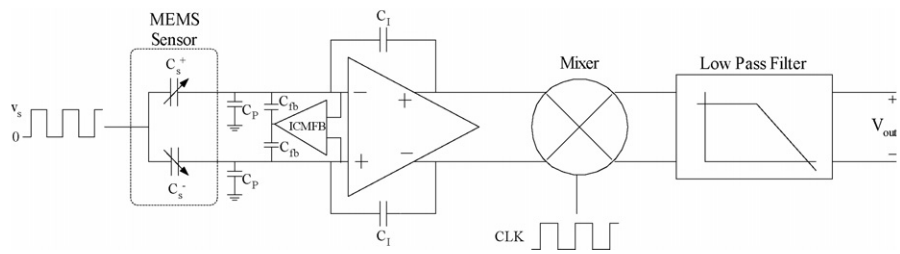

Fig. 9. Electronic strain sensing architecture.

gain of 19 and a sensitivity of 210 aF/microstrain with nonlinearity less than 0.5% FS were achieved, close to the FEA simulation (218 aF/microstrain) with a discrepancy less than 5%.

The device has also demonstrated a transverse strain rejection ratio of 100. A high resolution of 0.1 microstrain within the bandwidth from DC-10 kHz and a full range of ±1000 microstrains can be achieved with a matching interface circuit.

4. Interface electronics

The prototype electronic strain sensing architecture is presented in Fig. 9. The MEMS sensors, modeled as differential capacitors, are driven by a clock signal with amplitude of 3 V and are interfaced by a charge amplifier, which converts the sensor capacitance change to an output voltage. A clock frequency of 1 MHz is chosen to modulate the sensor information, and to shift away from the 1/*f* noise of the amplifier, a critical means to achieve a high sensitivity. The charge amplifier output is then mixed by the same clock signal and low-pass filtered to obtain the desired strain information. A second-order low-pass filter with a cut-off frequency of 150 kHz is designed to achieve a linear phase characteristic.

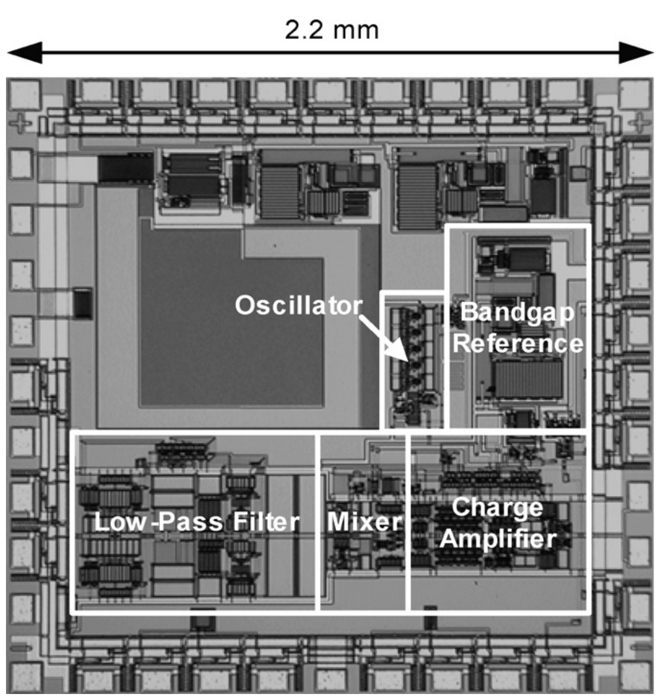

Fig. 10. Sensing electronics die photo.

A low noise charge amplifier with an input referred noise spectral density of 5 nV/(Hz)$^{1/2}$, is designed and fabricated using a 1.5 μm CMOS process and consumes 1.5 mA current from a 3 V supply. Fig. 10 shows the chip photo with the core interface electronics occupying an area of approximately 0.6 mm × 1.7 mm.

The MEMS sensor chip is first bonded to a stainless steel substrate and then wire bonded to the sensing electronics to form the prototype system and evaluated in the test set up. Fig. 11 shows the measured output voltage versus applied input strain, indicating that the system can achieve an input signal of ±1000 microstrains, corresponding to an output voltage of ±380 mV, with a linearity of 1.5% of full scale, and with a low noise level of 375 nV/(Hz)$^{1/2}$, equivalent to a resolution of 37.5 μV over 10 kHz bandwidth, thus a 80 dB dynamic range [7].

Fig. 12 is the RF powering architecture, where an external RF power source is used to drive a tuned series resonator consisting of $L_{B_{1B}}$ and $C_{B_{1B}}$ [8]. The resistor, $R_{B_{1B}}$, represents the overall series resistance associated with the resonator. The RF signal is coupled to a parallel resonator, consisting of L_2, and C_2, and a total loop resistance, $R_{B_{2B}}$, tuned to the same frequency. The signal is then rectified by an integrated CMOS fullwave rectifier to 5 V and further regulated to achieve a stable 3 V DC supply with a 2 mA current driving capability to power the sensor module.

An integrated CMOS fullwave rectifier used to rectify the received RF signal and convert it into DC is shown in Fig. 13,

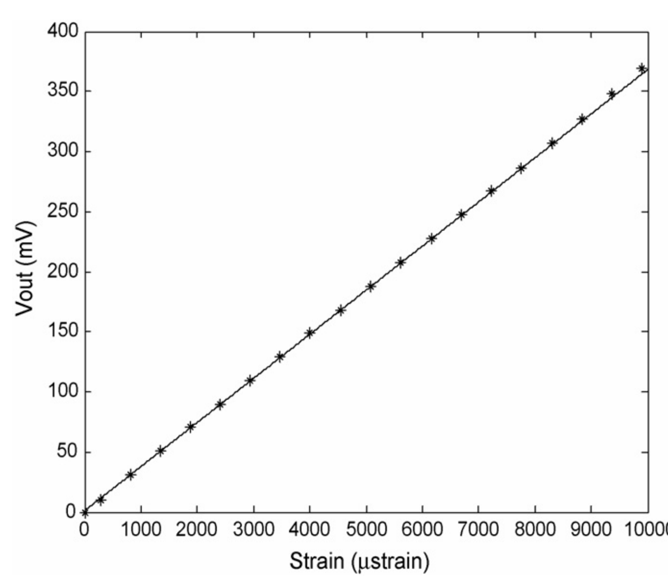

Fig. 11. Output voltage vs. input strain.

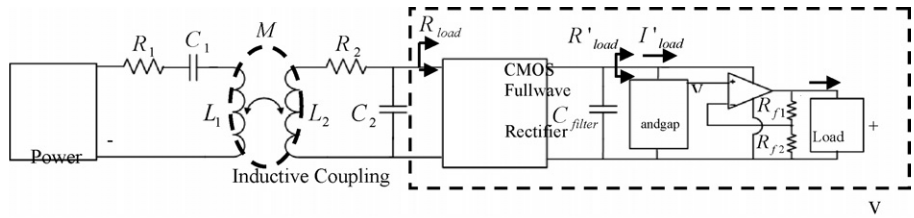

Fig. 12. The RF powering electronics architecture.

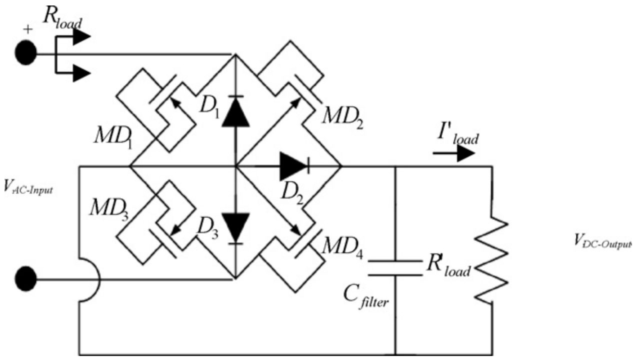

Fig. 13. The CMOS rectifying circuit.

where $V_{\text{AC-Input}}$ represents the coupled RF signal across the parallel resonator, which is rectified to produce a DC output voltage, $V_{\text{DC-Output}}$. The RF powering and signal telemetry unit was integrated onto the same chip of the interface electronics and is used to power the capacitive strain sensor and the low noise interface electronics. A strain resolution of 0.1 microstrains over a 10 kHz bandwidth and a dynamic range 80 dB were achieved. Which is the same performance achieved using 3 V battery.

5. Conclusion

The analysis, design, fabrication and evaluation of a high-performance capacitive strain sensor with low noise interface amplifier and RF powering electronics is presented. The work was carried out by a research team. The evaluated results on sensor modules fabricated agree well with the FEA simulation. These modules will be packaged for needed applications.

Acknowledgment

This work is supported by U.S. Army Research Office (ARO) under contract #DADD19-02-1-0198.

References

[1] M.L. Nagy, C. Apanius, J.W. Siekkinen, A user friendly, high-sensitivity strain gauge, Sensors 18 (June 2001) 20–27.

[2] M. Hrovat, D. Belavic, Z. Samardzija, J. Holc, An investigation of thick-film resistor, fired at different temperatures, for strain sensors, in: International Spring Seminar on Electronics Technology, May 2001, pp. 32–36.

[3] L.L. Chu, L. Que, M.-H. Li, Y.B. Gianchandani, Measurements of material properties using differential capacitive strain sensors, J. MEMS 11 (5) (October 2002), pp. 489–498.

[4] L. Lin, A.P. Pisano, R.T. Howe, A micro strain gauge with mechanical amplifier, J. MEMS 6 (4) (December 1997), pp. 313–321.

[5] J. Guo, H. Kuo, D.J. Young, W.H. Ko, Buckled beam linear output capacitive strain sensor, in: Solid-State Sensor, Actuator and Microsystems Workshop 2004 at Hilton Head, June 2004, pp. 399–403.

[6] H. Kuo, J. Guo, D.J. Young, W.H. Ko, Packaging of micro strain sensors, IEEE Sensors 2004, October 2004, pp. 546–549.

[7] M. Suster, J. Guo, N. Chaimanonart, W. Ko, D. Young, Low-noise CMOS integrated sensing electronics for capacitive MEMS strain sensors, in: IEEE Custom Integrated Circuits Conference, October 2004, pp. 693–696.

[8] N. Chaimanonart, W. Ko, D. Young, Remote RF powering system for MEMS strain sensors, in: Third IEEE International Conference on Sensors, Vienna, October 2004, pp. 1522–1525.

Biographies

Wen H. Ko received his BSEE from Xiamen University, China, in 1946, and his PhD degrees from Case Institute of Technology, Cleveland, Ohio, in 1959. He has been a faculty member of EE and BME Departments at Case Western Reserve University for 40 years. He is a professor Emeritus in EE of CWRU now.

Darrin J. Young received his BS with honors, MS, and PhD degrees from the Department of Electrical Engineering and Computer Sciences at University of California at Berkeley in 1991, 1993, and 1999, respectively. His doctoral dissertation emphasizes on microelectromechanical devices design and fabrication technologies for radio frequency analog signal processing. Between 1991 and 1993, he worked at Hewlett-Packard Laboratories in Palo Alto, CA, where he designed a shared memory system for a DSP-based multiprocessor architecture. During the summer of 1997, he worked at Rockwell Semiconductor Systems in Newport Beach, CA, where he designed silicon bipolar RF analog circuits for cellular telephony applications. Between 1997 and 1998, he was also at Lawrence Livermore National Laboratory, working on the design and fabrication of three-dimensional RF MEMS coil inductors for wireless communications. Dr. Young joined the Department of Electrical Engineering and Computer Science at Case Western Reserve University in 1999, where he is currently an associate professor. His research interests include MEMS and nano-electro-mechanical devices design, fabrication, and integrated analog circuits design for sensing, communication, biomedical implant, and general industrial applications.

Jun Guo received his BS degree from Tsinghua University, China, in 1993, and MS degree from Case Western Reserve University (CWRU) in 2000. From 2000 to 2002, he joined a telecommunication company where he was involved in designing MEMS wavelength optical switches and related high-voltage driving circuitry. Since 2002, he has been working towards his PhD degree at CWRU advised by Dr. Wen H. Ko. His current research activities are oriented towards the design, fabrication, and testing of MEMS physical sensors and nano-electro-mechanical devices for a variety of application fields.

Michael Suster received his BS and MS degrees in electrical engineering from Case Western Reserve University in 2002 and 2004, respectively. He is currently pursuing his PhD degree in electrical engineering at Case where he is a recipient of the Case Prime Fellowship. His current research interests include analog integrated circuit design for wireless MEMS sensors.

Hung-I Kuo received the BS degree in electrical engineering from Tatung Institute of Technology, Taipei, Taiwan, in 1992 and the MS and PhD degrees in electrical engineering and computer science from Case Western Reserve University, Cleveland, OH, in 1999 and 2002, respectively. His dissertation work focused on design, fabricate and testing MEMS devices based on 3C-silicon carbide on insulator substrates. Upon completion of the PhD program, he joined the Department of Electrical Engineering and Computer Science, Case Western Reserve University, Cleveland, OH, as research associate. He has 10 publications in journal/conference proceedings. His research interests include micro/nanofabrication technologies and packaging for MEMS devices.

Nattapon Chaimanonart received his bachelor degree in engineering from Electrical Engineering Department at Chulalongkorn University, Bangkok, Thailand, in 2001. Currently, he is now working toward his PhD degree at Case Western Reserve University in Cleveland, OH. Professor Darrin J. Young is his research advisor. His research interests are integrated-circuit design for wireless communications and interface electronics for biomedical sensing application.